academicJournals

Vol. 6(8), pp. 220-231, August, 2014
DOI: 10.5897/IJWREE2013.0489
Article Number: 1B02B2A46734
ISSN 2141-6613

http://www.academicjournals.org/IJWREE

International Journal of Water Resources and Environmental Engineering

*Full Length Research Paper*

# Transient numerical approach to estimate groundwater dewatering flow rates for a large construction site: a case study from the Middle East

**GUHA Hillol*, DAY Garrett and CLEMENTE José**

Bechtel Power Corporation, Geotechnical and Hydraulic Engineering Services, U.S.A.

Received 13 February, 2014; Accepted 9 June, 2014

**A three-dimensional, transient groundwater model was developed to determine the rate, volume, and number of pumping wells required to estimate the dewatering of three deep excavations at a large coastal construction site in the Middle East with a shallow groundwater table. There was limited site-specific hydrogeologic information for the site. A calibrated MODFLOW-based groundwater model was developed using the "the model-independent parameter estimation and uncertainty analysis" (PEST) software with pilot points and regularization mathematical techniques. Simulated heads were fitted against the monitoring well heads along extrapolated site groundwater head contours by estimating the hydraulic conductivity at each pilot point. Model-calibrated hydraulic conductivities obtained were within the range of medium to fine sand with silt values and matched closely with the subsurface material descriptions obtained through site geotechnical investigations. Dewatering of the three pits, each with approximate dimensions of 10 by 8 m and a depth of 20 m, was simulated through a series of sensitivity analyses to determine the number of wells, discharge rate, time duration to dewater the pits, and the volume of discharge water per pit to be diverted. Conclusions from the dewatering simulation estimations were as follows: (1) sensitivity analysis showed that the range of dewatering from each pit was dependent on the selected hydraulic conductivity and storage values, (2) storage was most sensitive to achieve the dewatered groundwater elevation depths, and (3) a one order-of-magnitude decrease of storage resulted in a shorter duration to dewater a pit. In summary, model simulations showed that site-specific pumping tests should be performed to optimize the design of a dewatering well system, specifically in low hydraulic conductivity soils where using large capacity wells is not feasible. The use of a numerical transient groundwater model is warranted for dewatering estimations as site-specific conditions are complex.**

**Key words:** Middle East, construction dewatering, groundwater modeling, MODFLOW, PEST.

## INTRODUCTION

Groundwater dewatering designs are often required prior to undertaking any subsurface geotechnical constructions (Ergun and Naicakan, 1993; Powers et al., 2007). The amount of dewatering is a function of the depth of the

*Corresponding author. E-mail: hguha@bechtel.com.

groundwater as it relates to the depth and size of the construction area (Powers et al., 2007; Preene, 2012). Understanding the geology, hydrogeology, and heterogeneity of the subsurface prior to undertaking dewatering is critical in successful geotechnical construction designs. Dewatering in a heterogeneous system requires development of a numerical groundwater model to better predict the number of well points or pumping wells required and also the time-variant nature of the dewatering process (Boak et al., 2007). We present a case study of a dewatering prediction rate estimate with the development of a numerical groundwater model of a large coastal construction site in the Middle East. The main objectives of this paper are to:

1. Develop a calibrated numerical groundwater model at and around three pits to include the site groundwater elevation shown in Figure 1 (determined from geotechnical boring logs and a limited number of groundwater observation wells) and
2. Estimate the rate, amount, and number of pumping wells needed to lower the groundwater elevation by approximately 20 m for each of the three pits with plan dimensions of approximately 10 by 8 m.

## METHODOLOGY

### Hydrogeological conditions

The study area is composed of Miocene and Pliocene sandy limestone, marl, gypsum, and beachrock formations. Evaporatic and low supratidal flats (Sabkha) are predominant and close to the study area. In the immediate study area geotechnical boring logs show interlayered medium to coarse sand with silt followed by thick fat clay layer at a depth of -21.5 m below ground surface. Groundwater elevation at the proposed dewatering area varied between 5 to 10 m below ground surface and is under unconfined condition, however, at greater depths groundwater is under confined conditions. Annual precipitation rates are very low along with high evaporation throughout the year result in a permanent water deficit. Although recharge is nearly zero due to high evaporation than precipitation; however, there are occasions when short heavy showers result in some recharge to the groundwater in similar hydrologic conditions (Memon et al., 1986; de Vries and Simmers, 2002; Kalbus et al., 2011).

### Groundwater model development

A three-dimensional numerical groundwater model was developed using the pre-processor Groundwater Vistas, version 5 (ESI, 2007), utilizing the U.S. geological survey MODFLOW 2000 numerical model code for groundwater flow. The model included two layers, a horizontal grid dimension of 10 by 10 m aligned in East–West and North–South directions, resulting in a total of 328 and 200 columns. The model dimension encompassed an area greater than that of the pit so as to minimize any modeled boundary effects near the pit dewatering area. The length and width of the model domain was 1,990 by 3,267 m, respectively. The average model vertical depth was approximately 27.6 m (elevation depth of -21.5 m) at the three dewatering pits. The two layers in the model were simulated as an unconfined aquifer as there were no confining lithologic units separating the two layers. The four boundaries of the model were depicted using the general head boundary (GHB) conditions (Figure 2). The GHB conductance was determined by multiplying the hydraulic conductivity of the layer with the area of the finite difference grid dimension of each cell and dividing by the thickness of the layer at each of the cell nodes corresponding to the GHB. As there was no surface water features or water level monitoring well outside the model domain, the immediate groundwater head assumed outside the model domain was based on the surface elevation (assuming that groundwater was at the surface).

The model was divided into two layers to differentiate between the two distinct lithologies as determined from the geotechnical boring logs. Based on the boring logs, the top layer was denoted as medium dense to dense sand with silt, and the lower layer was denoted very dense sand with silt. The boring logs indicated that at a depth of approximately -21.5 m elevation, hard, fat clay exists at the pit area. As there were limited boring logs within the model domain, the existence and depth of the clay layer beyond the pit areas was not certain. For the purpose of model development, the clay layer was assumed to exist within the model domain. The clay layer was assumed as no-flow boundary within the model domain. The surface elevation of the model varied between 0.35 to 13 m, whereas, in the immediate project area, the range of surface elevation was 4.5 to 7 m. The thicknesses of model layer 1 varied between 0.5 to 9 m, and for layer 2, the thickness varied between 18 and 26 m. The model did not include any net recharge as it was assumed that groundwater infiltration was minimal and did not significantly impact the site.

### Groundwater model calibration

The numerical groundwater model was calibrated under steady-state conditions, using the groundwater head contour distribution, as shown in Figure 1, as the target heads. The target heads were distributed along the contours in Figure 1. MODFLOW 2000 code was used to simulate the groundwater heads (Harbaugh et al., 2000). Prior to performing the calibration run, a total of 426 hydraulic conductivity pilot points were distributed within the model domain (Figure 2). These pilot points were distributed uniformly outside the immediate area of the project area but were increased in the area where the groundwater head contours are shown in Figure 1. The model-independent parameter estimation and uncertainty analysis (PEST) software with pilot point and regularizations (Doherty, 2010; Watermark Numerical Computing, 2010) was used to calibrate the model by fitting the simulated head against the monitoring well heads by estimating the hydraulic conductivity at each pilot point. Hydraulic conductivity was distributed among the pilot points using the Kriging interpolation method of geostatistics (Watermark Numerical Computing, 2010).

The regularization approach provides an advantage in estimating more parameters than there are observations to calibrate against. It is also a technique in minimizing the global objective function ($\phi_g$). The global objective function can be defined as:

$$\phi_g = \phi_m + \mu\phi_r \quad (1)$$

where $\phi_m$ is the measurement objective function, $\phi_r$ is the regularized objective function, and $\mu$ is similar to a Lagrange multiplier, which in PEST is estimated through the Gauss-Marquadt-Levenberg optimization routine (Doherty, 2010).

The measurement objective function, $\phi_m$, is defined as

$$\phi_m = (d - M(p))^t Q_1 (d - M(p)) \quad (2)$$

where *d* represents vector of field measurement, *M* is the modeled simulated values, $Q_1$ is the weight of the observation points, and

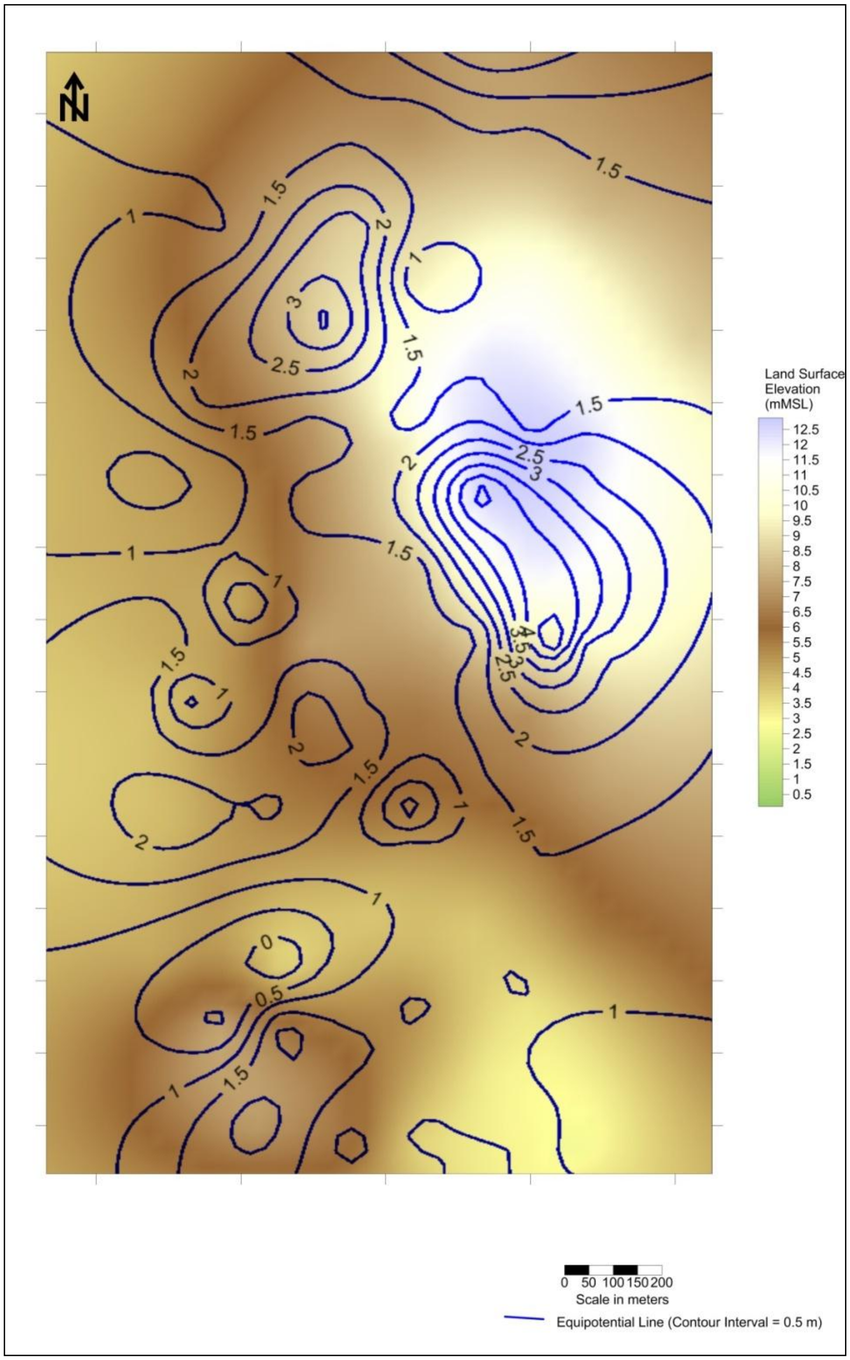


**Figure 1.** Site Observed Groundwater Levels

*d–M(p)* is the difference between field and modeled data acting on parameter vector p.

The regularized objective function, $\phi_r$, is defined as

$$\phi_r = (e - R(p))^t Q_2 (e - R(p)) \quad (3)$$

where *e* is the regularized observation values, *R* is a regularized operator acting on the parameter vector *p*, $Q_2$ is the weights assigned to the regularized observations, and *e–R(p)* is the difference between regularization observation and regularized parameter vector values.

Figure 3 shows the simulated groundwater head distributions within the model domain under steady-state conditions. Figure 4 shows the simulated groundwater head distribution at and around the three-pit area. The distribution of the simulated groundwater heads was within 0.1 m of the measured heads (Figure 1) at the dewatering area and outside; that is, in areas to the northeast of the model domain, it varied between 0.5 and 1 m. The greater

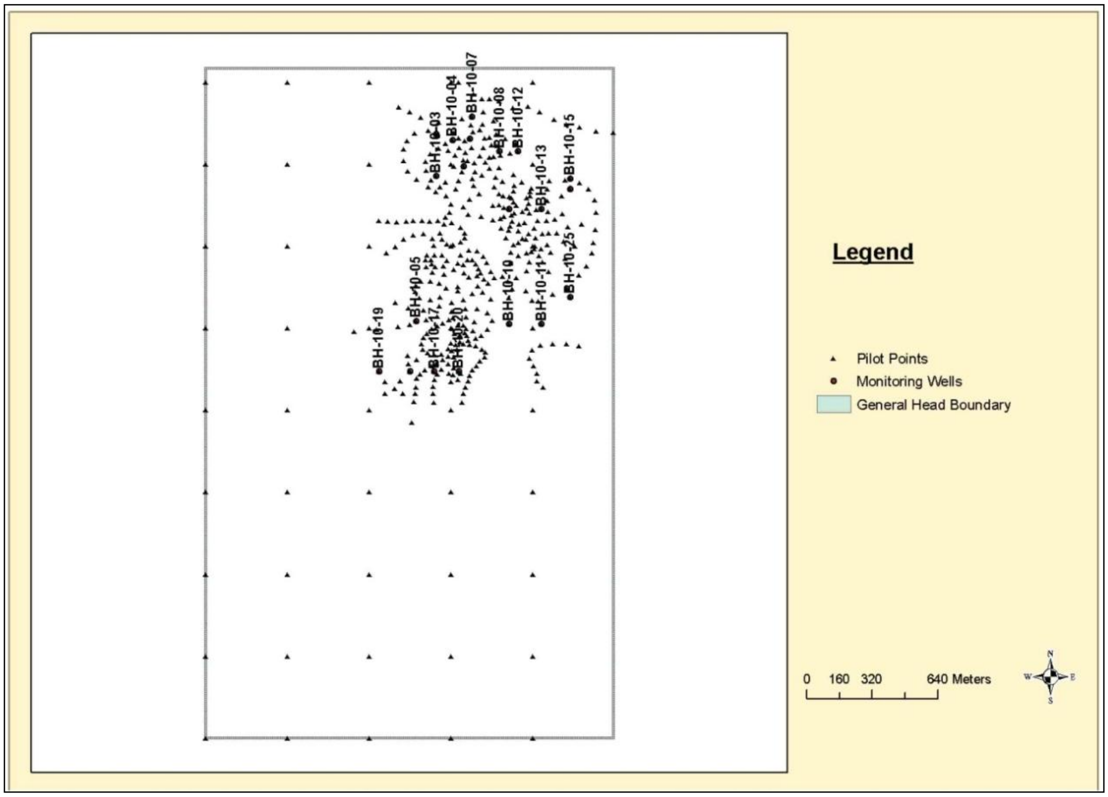


**Figure 2.** Model domain and pilot points distributions.

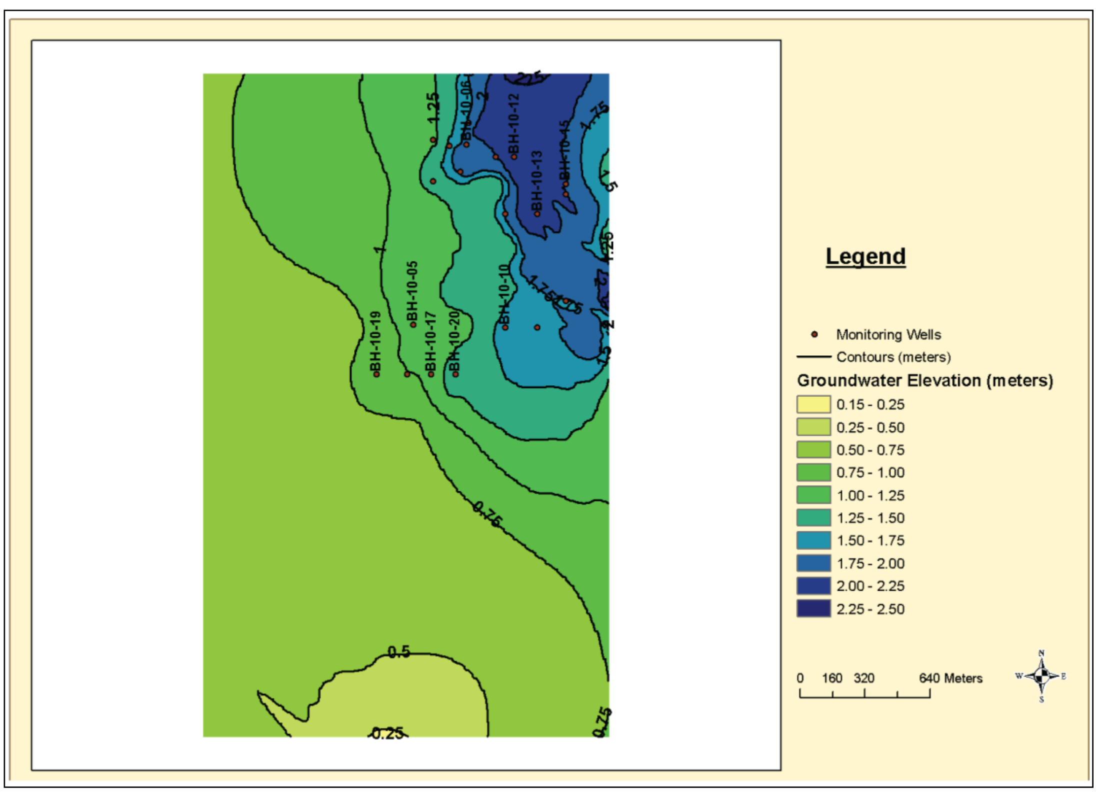


**Figure 3.** Groundwater head contours in the Calibrated Groundwater Model.

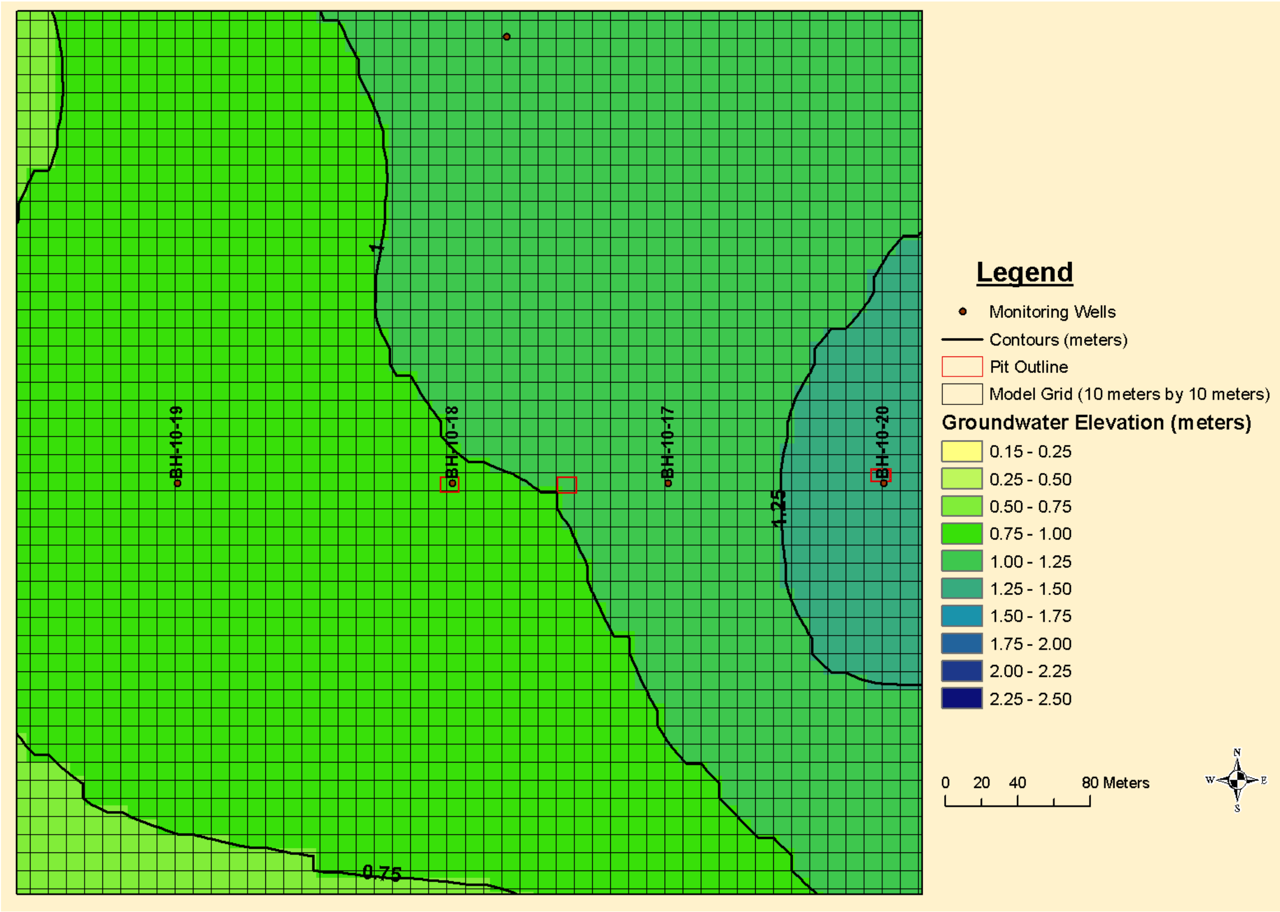


**Figure 4.** Groundwater head contours in the Calibrated Groundwater Model in the pit areas.

difference in heads between contoured heads (Figure 1) with that of the simulated head in the northeastern portion of the model domain was attributed to hydrogeologic conditions that may not be correctly conceptualized in the current groundwater model. However, the model-simulated heads did capture the mounding effects to the northeast. Some boundary effect is also responsible for the difference in the heads in the northeast portion of the model; however, the effects of the boundary did not have any impact at and around the three-pit area.

Figures 5 and 6 show the calibrated horizontal and vertical hydraulic conductivity distributions in layer 1 at the proposed dewatering zone. Similarly, Figure 7 depicts the calibrated horizontal hydraulic conductivity distributions in layer 2. The vertical hydraulic conductivity of layer 2 was $1.2 \times 10^{-5}$ cm/s. The values of the horizontal hydraulic conductivity distributions were within the range of the medium to fine sand with silt values as provided in Table 4.6 of Fetter (1994). The estimated hydraulic conductivity values were determined inversely (no trial-and-error approach) by the model-independent parameter estimation and uncertainty analysis (PEST) suite of algorithms and the values are within the reported values of the lithologic units. The vertical hydraulic conductivity values were, on average, an order of magnitude smaller than the horizontal hydraulic conductivity values. Layer 1, which was described as medium dense to dense sand with silt, was characterized by horizontal hydraulic conductivities ranging from $1.1 \times 10^{-4}$ cm/s to $1.5 \times 10^{-3}$ cm/s at and around the three pits (Figure 5). The higher values of horizontal hydraulic conductivities than the vertical hydraulic conductivities is attributed to the anisotropy of the soil types, where the dominant flow is along the horizontal direction which is typical in this kind of hydrogeological settings. In layer 2, the horizontal hydraulic conductivity values at and around the three pit areas were mostly within the range of $1.1 \times 10^{-4}$ cm/s to $4.4 \times 10^{-4}$ cm/s; in the immediate area of Pit 3, however, the value ranged from $1.3 \times 10^{-3}$ cm/s to $4.6 \times 10^{-3}$ cm/s (Figure 7).

## RESULTS AND DISCUSSION

### Pits dewatering estimate

Once the groundwater model was calibrated against the groundwater heads, the next step was to estimate dewatering rates for the three pits (Figure 4). Pits 1 and 2 were defined by a surface perimeter of approximately 10 by 8 m, and Pit 3 was approximately 10 by 7 m. Because the grid dimensions of the calibrated model were 10 by 10 m, finer grid discretization of 0.5 by 0.5 m was utilized at and around the three pits to numerically estimate the required dewatering at the pits. The grid was also expanded at selected areas beyond the vicinity of the pit. The maximum grid dimensions in the finer resolution model were 14 by 14 m. The total number of rows and

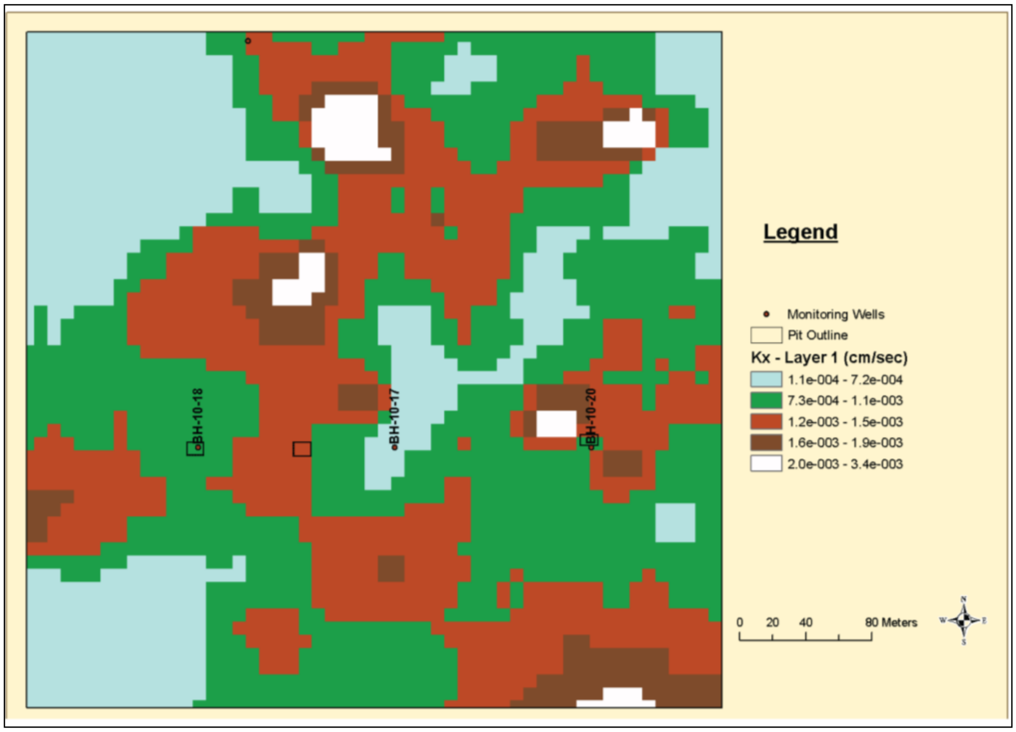


**Figure 5.** Distribution of Horizontal Hydraulic Conductivity Values in Layer 1 of the Groundwater Model at the pit areas.

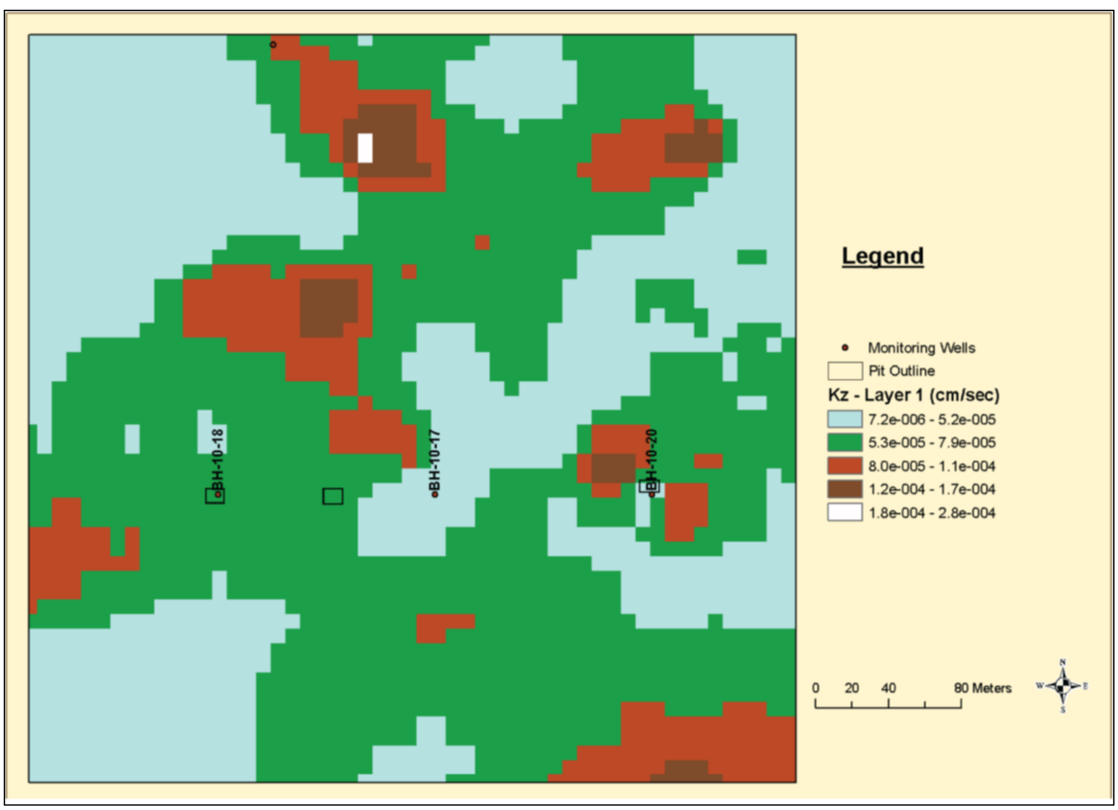


**Figure 6.** Distribution of Vertical Hydraulic Conductivity Values in Layer 1 of the Groundwater Model at the pit areas.

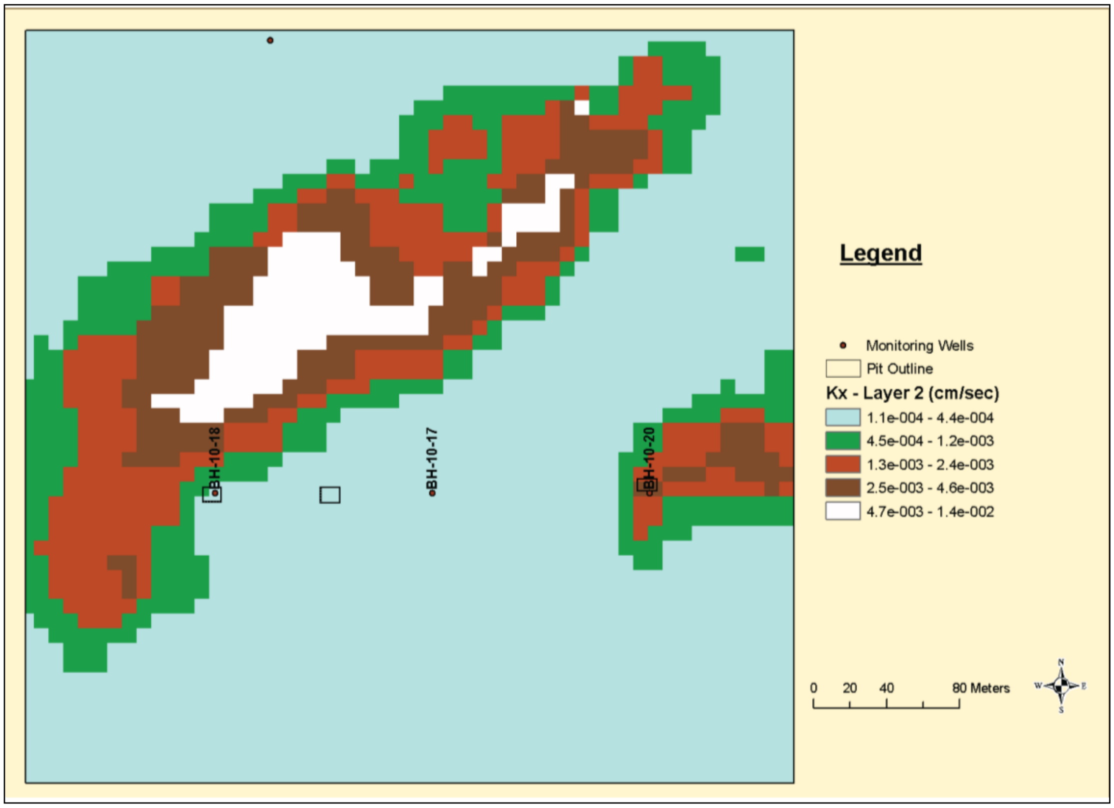


**Figure 7.** Distribution of Horizontal Hydraulic Conductivity Values in Layer 2 of the Groundwater Model at the pit areas.

columns in the model was 524 and 947, respectively. A steady-state simulation of the finer resolution model was run to compare the groundwater heads with those of the 10 by 10 m grid dimension model. The results of the heads compared satisfactorily within the model domain.

The three pits were dewatered in order, starting with pit 1, followed by pit 2 and then, ultimately, pit 3. It was assumed that once each pit was dewatered, concrete would be poured in each pit for construction (base and side walls). In the groundwater model, the pit area that had been dewatered was simulated as a no-flow zone for the next pit dewatering simulation. It was assumed that during the dewatering process, there was no rainfall at the site, and groundwater pumped from the pit was discharged offsite to avoid recharging the aquifer in the immediate area of the three pits.

Pit dewatering was simulated by pumping from wells along the perimeter of each pit. The wells were spaced at distances of approximately 1 m from each other. The number of wells, pumping rate, depth, and location of the wells are shown in Table 1. As dewatering is a transient process, aquifer storage terms were represented uniformly within each of the two layers. For layers 1 and 2, specific yield values of 0.21 and 0.18, respectively, were selected. These are average values for fine sand and silt as stated in Table 4.4 of Fetter (1994). The selection of the pumping rate of each well at 19.1 $m^3$/day was arbitrary and was based on experience with dewatering in such geologic settings. However, the grain size analysis data show that the sediments at the site are tight, and thus, higher pumping rates may not be feasible. Prior to beginning any field dewatering activities, an aquifer test including step-test analysis for well pumping should be undertaken to estimate the most feasible rate of groundwater pumping.

### Pit 1 dewatering rates

A total of 34 pumping wells, each pumping at 19.1 $m^3$/day, were distributed along the perimeter of the pit. Pumping proceeded for a total of 30 days before the groundwater head decreased to a level of approximately -18.5 m elevation. Figure 8 shows the time versus head and discharge in the location of the center of pit 1. The total water discharged at the end of the 30 days of pumping was approximately 8,500 $m^3$.

### Pit 2 dewatering rates

Prior to simulating dewatering at pit 2, the area of pit 1 was simulated as a no-flow zone (to mimic the construction of the pit). The configuration and rate of the

**Table 1.** Pumping Well Information Used in the Groundwater Model.

| Pit | Number of wells | Pumping rate of each well (gpm) | *Well screen elevation (m - msl) | Locations of wells |
|---|---|---|---|---|
| 1 | 34 | 3.5 | 6.2 to -20 | Along the perimeter of the pit |
| 2 | 34 | 3.5 | 6.2 to -20 | Along the perimeter of the pit |
| 3 | 36 | 3.5 | 6.2 to -20 | Along the perimeter of the pit |

* The well screen elevation is based on aquifer depth identified in the groundwater model. For actual dewatering at the site, the well screen depth may vary depending on actual site hydrogeologic conditions encountered.

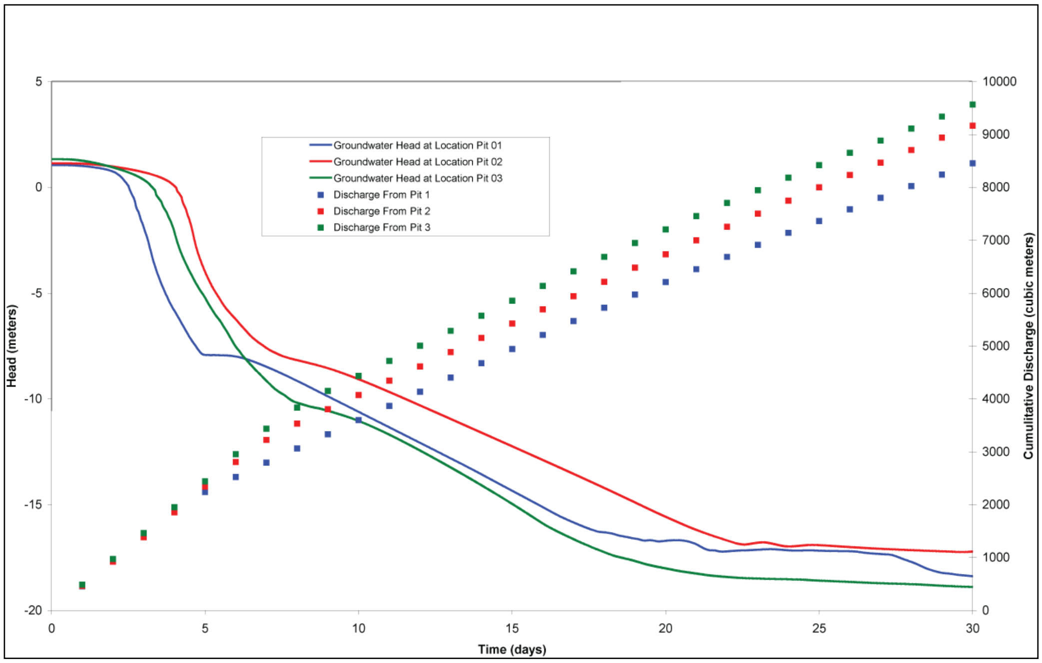


**Figure 8.** Groundwater Head and cumulative discharge with time for the three pits.

pumping wells were similar to those in the dewatering of Pit 1. Pit 2 was also dewatered for 30 days, with the groundwater head elevation decreasing to approximately -17.3 m at the target location in Pit 2 (Figure 8). The failure to reach the target elevation depth of -18.5 m after 30 days was attributed to a few dry wells and also to the lower hydraulic conductivities in the area of Pit 2. It is expected that sump pumps could be used in the bottom of the excavation to lower the groundwater head an additional meter to the target elevation. After 30 days of pumping, the total discharge from Pit 2 was approximately 9,200 $m^3$.

## Pit 3 dewatering rates

Pit 3 was dewatered with a total of 36 pumping wells, each discharging at 19.1 $m^3$/day. The two additional wells in Pit 3 were the result of the slightly different pit outline and the fact that the initial groundwater table was higher than the level of the other two pits. Figure 8 shows the relationship between time and groundwater heads and discharge at Pit 3. The total groundwater discharge from Pit 3 at the end of 30 days of pumping was approximately 9,600 $m^3$. Pits 1 and 2 were simulated as no-flow boundary conditions to represent post-construction conditions.

## Sensitivity analysis

To determine the impact that the hydraulic conductivity and storage values have on dewatering estimates for the three pits, a series of sensitivity analyses were conducted. Pumping rates were similar to the rates used in the dewatering of Pits 1, 2, and 3 as already discussed under “Pit dewatering estimate” above. The sensitivity analyses included:

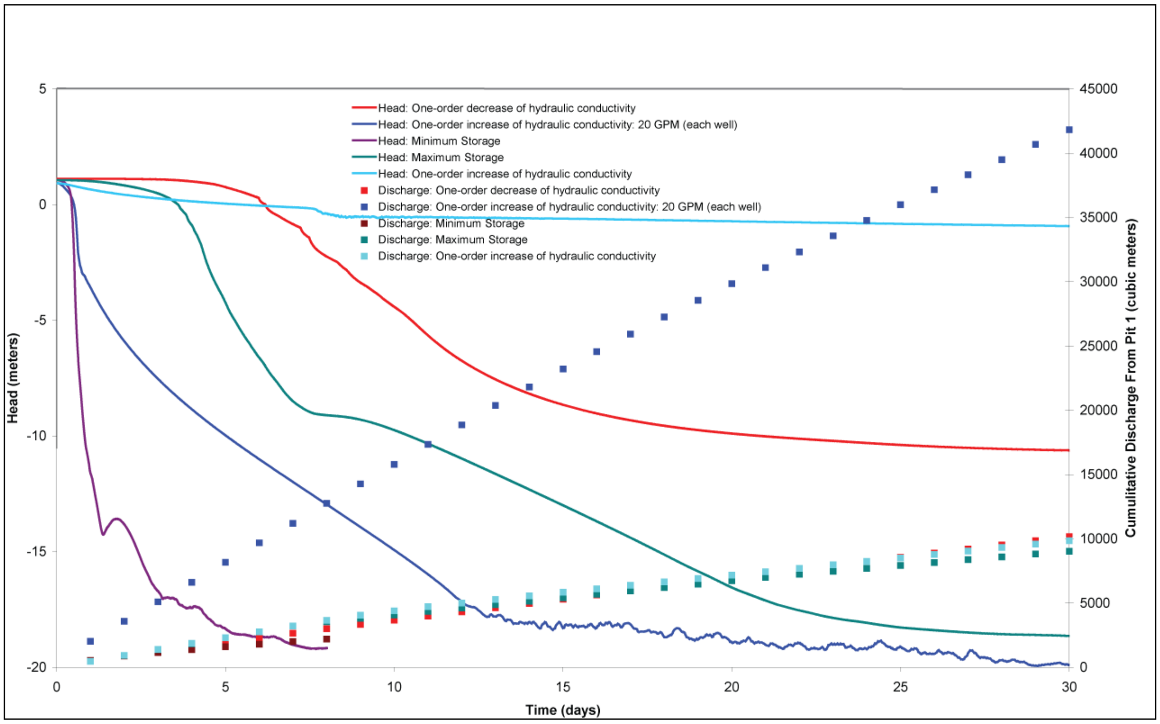


**Figure 9.** Sensitivity of Groundwater Head and cumulative discharge with time for Pit 1.

1. Increase of hydraulic conductivity (both horizontal and vertical) by one order of magnitude from the calibrated model values;
2. Decrease of hydraulic conductivity (both horizontal and vertical) by one order of magnitude from the calibrated model values;
3. Minimum storage (specific yield) values for fine sand (layer 1 in the model) and silt (layer 2 in the model) of 0.1 and 0.03, respectively; these values are shown in Table 4.4 of Fetter (1994) and
4. Maximum storage (specific yield) values for fine sand (layer 1 in the model) and silt (layer 2 in the model) of 0.28 and 0.19, respectively; these values are shown in Table 4.4 of Fetter (1994) Figures 9 to 11 show plots of time versus groundwater head and discharge for Pits 1, 2, and 3, respectively.

### *Pit 1 sensitivity analyses*

Increasing the hydraulic conductivities by one order of magnitude resulted in very minimal groundwater dewatering (lowering of the groundwater elevation to -1.0 m) after 30 days of pumping. However, increasing the pumping rate of the individual wells from 19.1 to 109 $m^3$/day lowered the groundwater head to an elevation of -18.5 m within 15 days of pumping; however, pit dewatering reached a depth elevation of -20 m until 30 days of pumping. Although the required simulated depth of dewatering was achieved within 15 days of the start of pumping, it took another 15 days to achieve an extra 1.5 m (that is, to -20 m elevation) due to the groundwater fluctuations occurring very close to the fat clay below layer 2. The total groundwater discharge after 30 days with pumping rate of 109 $m^3$/day from each well was approximately 42,000 $m^3$ (Figure 9).

Decreasing the hydraulic conductivity by one order of magnitude resulted in a groundwater elevation at the pit after 30 days of pumping of about -10.5 m elevation. The total groundwater discharge after 30 days was about 10,000 $m^3$. Due to lower hydraulic conductivities (one order-of-magnitude decrease from calibrated values), the model showed that it will take more time (that is, more than 30 days pumping at a rate of 19.1 $m^3$/day) to lower groundwater heads at Pit 1 to a target elevation of -18.5 m.

Groundwater storage played a greater role in the estimate of groundwater heads with time during dewatering. Decreasing the groundwater storage (that is, specific yield) to 0.1 and 0.03 in layers 1 and 2, respectively, yielded faster pit dewatering. The model sensitivity run showed that Pit 1 achieved the target dewatering elevation of -18.5 m within 6 days of pumping. The total groundwater discharged after 6 days of dewatering was approximately 1,800 $m^3$. When specific yield values were increased to 0.28 and 0.19 for layers 1 and 2, groundwater heads reached the dewatering target of -18.5 m elevation within 28 days. The total groundwater discharged after 28 days was approximately 8,600 $m^3$.

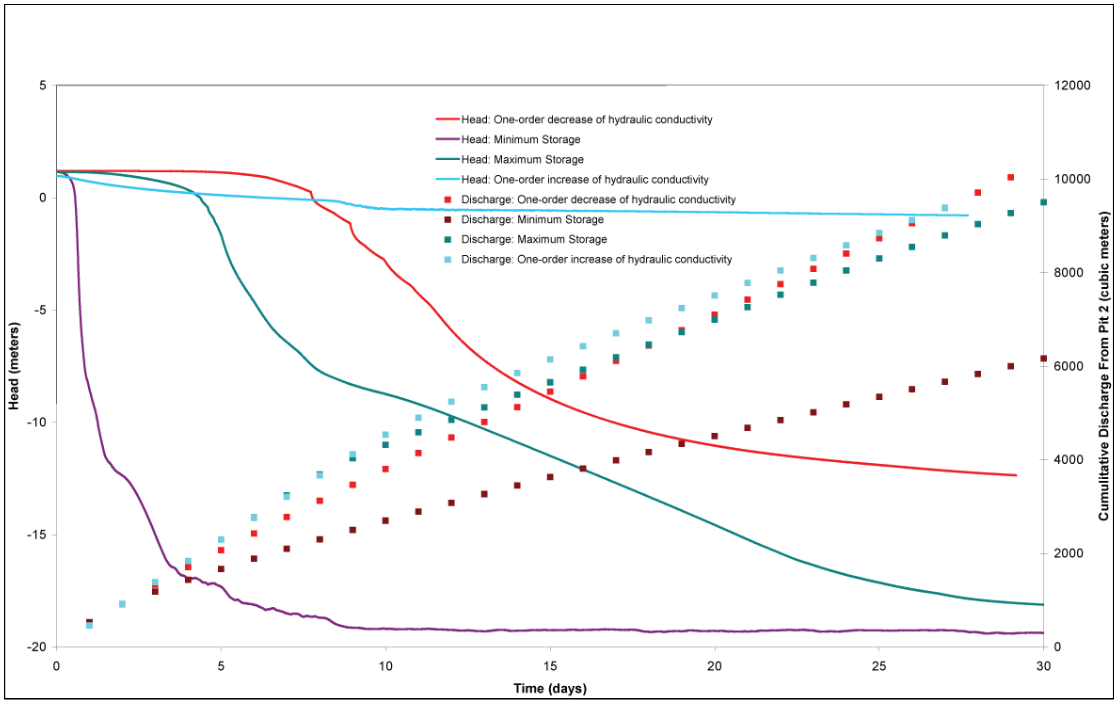


**Figure 10.** Sensitivity of Groundwater Head and Cumulative Discharge with Time for Pit 2.

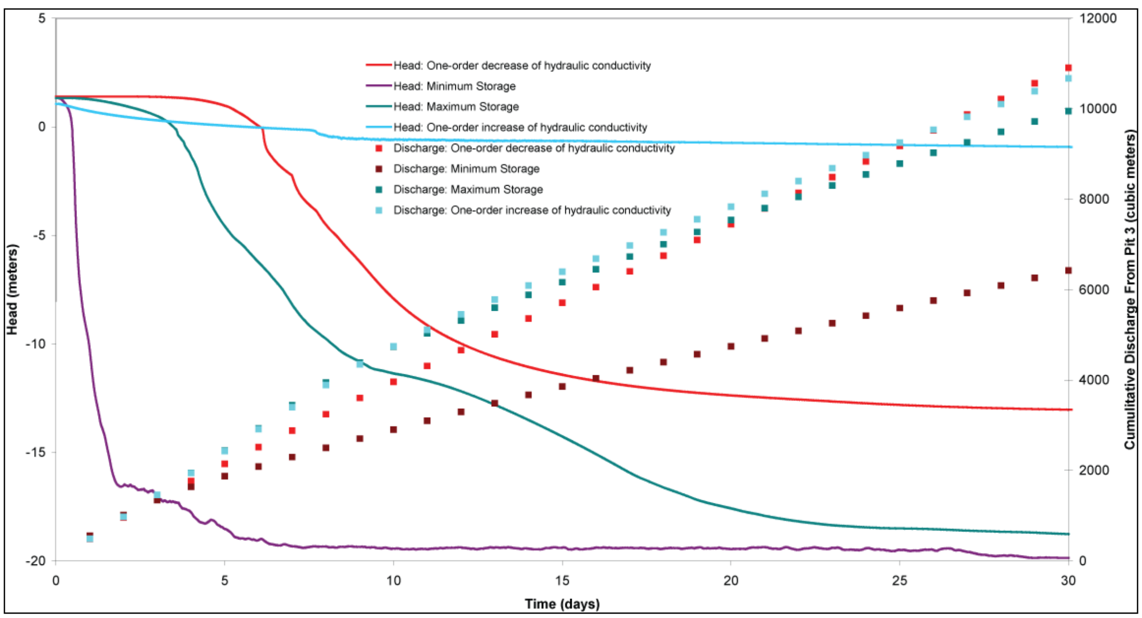


**Figure 11.** Sensitivity of Groundwater Head and Cumulative Discharge with Time for Pit 3.

***Pit 2 sensitivity analyses***

Pit 2 sensitivity analyses were conducted under conditions similar to the Pit 1 sensitivity analyses. The results of increasing and decreasing the hydraulic conductivity and storage values were similar to those in the Pit 1 sensitivity analyses (Figure 10).

***Pit 3 sensitivity analyses***

Pit 3 sensitivity analyses were conducted under conditions similar to the Pits 1 and 2 analyses. The results of increasing and decreasing the hydraulic conductivity and storage values were similar to the results from the Pits 1 and 2 sensitivity analyses (Figure 11). The sensitivity analyses show that a one order-of-magnitude increase of hydraulic conductivities above the calibrated hydraulic conductivity values will require a longer time to achieve the target dewatering elevation of -18.5 m, with approximately 34 to 36 wells pumping at a rate of 19.1 $m^3$/day. However, if the pumping rates for the individual wells are increased to 109 $m^3$/day, then it is possible to achieve the target dewatered elevation depth for the pits, as shown in the sensitivity analysis of pit 1. Storage plays a large role in dewatering estimation; a slight increase or decrease of storage impacts the time it takes to reach the groundwater level dewatering target. The lower the storage values for the sediments, the faster the groundwater dewatering target elevation is attained.

## Assumptions

The following assumptions were used to evaluate the groundwater dewatering heads in the model:

1. The groundwater at the site represents uniform density;
2. There is no tidal influx affecting the dewatering pits;
3. The hydraulic conductivity and storage used in the model represent the values at the site;
4. There is no recharge during the dewatering processes;
5. Lithologic and groundwater information in the model at distances away from the pit areas is not ascertained from the available geotechnical field investigations and
6. Pumping rates used in the calculation during dewatering are constant. Initial water levels prior to dewatering of the pits are similar to those shown in Figure 1.

## Conclusions

A groundwater model was developed for the purpose of estimating both the dewatering rates and the volume of groundwater that required removal from the three pits to achieve a construction dewatering groundwater elevation of -18.5 m. The model was calibrated against estimated maximum observed groundwater heads at the area of the pits. The estimated range of hydraulic conductivities was based on the lithologies from the geotechnical borehole logs. Dewatering of the three pits was evaluated by performing model simulations, starting with Pit 1, then Pit 2, and lastly, Pit 3. For Pit 1 dewatering, a total of 34 pumping wells, each pumping at 19.1 $m^3$/day for 30 days, were simulated until the target elevation was reached. The pumping wells were distributed along the periphery of the pit. The same well configuration was used to simulate dewatering at Pit 2. For Pit 3, 36 pumping wells were used because the pit outline (perimeter) is slightly different than those of Pits 1 and 2. In addition, the preconstruction dewatering groundwater heads at Pit 3 are slightly higher than the heads at Pits 1 and 2. The approximate total amount of water diverted to lower the dewatered groundwater elevation for each pit to -18.5 m was about 9,500 $m^3$. This estimation was based on model simulation values.

A series of sensitivity analyses were conducted to determine the effects of increasing and decreasing aquifer hydraulic conductivities and storage values on the dewatering estimates. The sensitivity analyses show that a one order-of-magnitude increase of hydraulic conductivity above the calibrated values would require more than 30 days of pumping to achieve the target dewatering depth. However, if the pumping rate was increased from 19.1 to 109 $m^3$/day for each of the 34 wells, the target depth of -18.5 m would be achieved within 15 days. Decreasing the hydraulic conductivity by one order of magnitude shows that the groundwater target depth is not achieved within the 30 days. Complete dewatering will require more time if the pumping rate from each well remains at 19.1 $m^3$/day.

Storage (or specific yield) values have a significant impact on the dewatered groundwater elevation depths. Decreasing the specific yield to 0.1 and 0.03 for layers 1 and 2 caused the groundwater elevation at the Pits to reach the target dewatered elevation within 6 days. Increasing the specific yield to 0.28 and 0.19 for layers 1 and 2 showed that the time to achieve the target elevation was approximately 28 days. The sensitivity analyses show that the range of total water dewatered from each pit depends on the selected hydraulic conductivity and storage values and varies from approximately 9,000 to 27,000 $m^3$ (for a one order-of-magnitude increase of hydraulic conductivity with a 109 $m^3$/day pumpage from each well) to achieve the target dewatered elevation of -18.5 m.

The model results show that it is possible to dewater the three pits using groundwater wells; however, specific information of dewatering pumping rates needs to be deciphered from site-specific pumping tests (step and constant rate discharge tests) to determine the hydrogeologic properties. The actual amount of water discharged will also depend on groundwater level conditions at the site. The current groundwater model is a planning-level tool to estimate dewatering potential at the three pits; however, for project design, site-specific information such as pumping tests should be performed to better estimate the site's dewatering capability. The number of wells used for dewatering simulations is not expected to be the exact number that is required for the actual dewatering process. For a required inflow into an excavation, there is more than one potential solution; a greater number of smaller wells, for example, achieve the same results as a smaller number of larger, higher-volume wells.

It is therefore recommended that a pumping test (step and constant rate discharge tests) be performed at any one of the pit areas. The tests would further determine how much water can be diverted from each well and would fine-tune the well pumping rate. The rate of flow into a pumped well or well point depends on the area and permeability of the ground immediately outside the well and on the hydraulic gradient causing the flow. Evaluation of the pumping test would provide a refined estimate of average hydraulic conductivity and storage of the pumping domain. The groundwater model would then be refined to better estimate the dewatering rates.

If the site step tests and pumping tests show that each of the individual wells can be pumped at rates greater than 19.1 $m^3$/day, then the groundwater model would be run with the new pumping rate. The model would help determine the required number of wells needed and the placement of the wells before groundwater dewatering is initiated. Additional dewatering methodologies should also be considered, including a series of well points, sumps, and/or cutoff walls and depends on the hydraulic conductivity and storage values determined from site-specific pumping tests.

**REFERENCES**

Boak R, Bellis L, Low R, Mitchell R, Hayes P, McKelvey P, Neale S (2007). Hydrogeological impact appraisal for dewatering abstractions. Science Report – SC040020/SR1. U.K. Environmental Agency. ISBN: 978-1-84432-673-0.

Doherty J (2010). Addendum to the PEST Manual. Watermark Numerical Computing, Revision: September 2010.

de Vries JJ, Simmers I (2002). Groundwater recharge: an overview of processes and challenges. Hydrogeol. J. 10:5-17.

Environmental Simulations, Inc. (2007). Guide to Using Groundwater Vistas Version 5, Reinholds, PA.

Ergun MU, Naicakan MS (1993). Dewatering of a Large Excavation Pit by Wellpoints, Third International Conference on Case Histories in Geotechnical Engineering, St Louis, Missouri, 1993, Paper No. 5.12.

Fetter CW (1994). Applied Hydrogeology, Third Edition, 1-691.

Harbaugh AW, Banta ER, Hill MC, McDonald MG (2000). MODFLOW-2000, The U.S. Geological Survey Modular Ground-water Model-User Guide to Modularization Concepts and the Ground-Water Flow Process: U.S. Geological Survey Open-File Report 00-92, 1-121.

Kalbus E, Oswald S, Wang W, Kolditz O, Engelhardt I, Al-Saud MI, Rausch R (2011). Large-scale Modeling of the Groundwater Resources on the Arabian Platform. Int. J. Water Res. Arid Environ. 1(1):38-47.

Memon BA, Kazi A, Powell WJ, Bazuhair AS (1986). Estimation of Groundwater Recharge in Wadi Al-Yammaniyah, Saudi Arabia. Environ. Geol. Water Sci. 8(3):153-160.

Powers PJ, Corwin AB, Schmall PC, Kaeck WE (2007). Construction Dewatering and Groundwater Control: New Methods and Applications, Third Edition. John Wiley & Sons, Inc. ISBN: 9780471479437.

Preene M (2012). Groundwater Lowering in Construction: A Practical Guide to Dewatering, Second Edition. CRC Press, 673 pp.

Watermark Numerical Computing (2010). *PEST:* Model-Independent Parameter Estimation, User Manual*:* 5th Edition.